Article:
Ishizaka, K., White, B., Watson, M. et al. (2020) Influence of temperature on adhesion coefficient and bonding strength of leaf films: a twin disc study. Wear, 454-455. 203330. ISSN: 0043-1648

https://doi.org/10.1016/j.wear.2020.203330

Influence of temperature on adhesion coefficient and bonding strength of leaf films: a twin disc study

Kei Ishizaka [a, b], Benjamin White [a], Michael Watson [a], Stephen R Lewis [a, c] and Roger Lewis [a]

[a] Department of Mechanical Engineering, The University of Sheffield, Mappin Street, Sheffield S1 3JD, UK

[b] East Japan Railway Company, 2-2-2 Yoyogi, Shibuya-ku, Tokyo 151-0053, Japan

[c] British Steel, Scunthorpe Rail and Section Mill, Brigg Road, Scunthorpe, DN16 1BP

Corresponding author: Roger Lewis

Email: roger.lewis@sheffield.ac.uk

Address: Department of Mechanical Engineering, The University of Sheffield, Mappin Street, Sheffield S1 3JD, UK

Tel: +44 (0) 114 222 7838

Fax: +44 (0) 114 222 7890

Abstract

In the autumn, train operations in the UK are likely to be unstable due to the low adhesion coefficient between the wheel and rail, and fallen leaves on the line have been known as the main cause of this problem. In this study, the temperature effects on the adhesion coefficient as well as the bonding strength of the leaf film were investigated using a twin disc machine, to develop a potential prevention and mitigation method. The high surface temperature of the disc seemed to improve the adhesion when the leaf powder suspension was present, forming a linear relationship between the surface temperature. The surface temperature around 240 °C could be enough to attain the required level of traction. The high temperature could decrease the bonding energy between the leaf film and rail, possibly decelerating the chemical reaction for the leaf film formation. Continuous drag braking in the autumn was proposed as a countermeasure. Two effects can be expected for this method: prevention of leaf contamination by removing the leaf residue on the wheel surface and improvement of the adhesion level by braking heat.

Keywords: Low adhesion; Leaf contamination; Leaf film; Twin disc; Scratch test; Heat application; Raman spectroscopy; Fourier transform infrared spectroscopy; Drag braking

1. Introduction

Fallen leaves on the line are one of the main concerns for railway industries in the autumn; they contaminate the rail surface and lower the friction between the wheel and rail, which is usually called “adhesion” in this field (1–3). When low adhesion is forecast or occurs, train operating companies are frequently subjected to amended timetables, delays and occasional cancellations to guarantee safety as well as minimum transportation. However, this status is undesirable for railway industries; it leads to a decrease in ticket sales, customer satisfaction and most importantly, social credibility of railway transportation. Hence, this leaf contamination problem should be resolved to attain safe and stable train operation for train users.

Leaves form a black and slippery “leaf film” on the rail surface after being crushed by passing wheels, and this leaf film is known to cause low adhesion. To overcome the low adhesion in the autumn, two measures are currently employed in the UK: traction enhancer and water-jet cleaning by a special train called a Rail Head Treatment Train (RHTT) (4). Traction enhancers and RHTTs can be effective in removing leaf films; however, overuse of traction enhancers (mostly sand) can lead to damages and higher wear rates of both a wheel and rail due to the abrasive nature of the particles (5–8). Operation of the RHTT also incurs additional costs (9), and the RHTT has been reported to travel more than four times around the world in just one operating season in the UK (10). For further reduction in operating costs, it is crucial to minimise the use of traction enhancer and water-jet cleaning.

From the viewpoint of train operation management, prevention of the leaf film formation should be considered in the first place. There are some prevention methods, including the pH value control on railheads (11). However, this prevention method was empirically introduced, and the mechanism of the prevention has not yet been clarified due to the lack of understanding regarding the chemical reaction between leaf organics and rail steels. Another and better prevention method could be developed if the chemical reaction process is determined.

Recent research by the authors found that water-soluble organics of leaves react with rail steels and form a black material, which shows lower friction than engine oil (12). Chemical analysis suggests that some organic acids in leaves trigger the chemical reaction and help to dissolve the rail steel and form an iron carboxylate or iron oxide core. Based on this theory, a new prevention method has been proposed: heat application to the contact area.

In general, organic acids can decompose under medium-high temperature. For example, gallic acids, which are one of the candidates for the chemical reaction, have been reported to decompose around 150 °C in an aqueous solution, although the decomposition time is hourly (13). If the organic acids are broken down, they cannot help dissolve the rail steel, and thus, a black material should not be formed. This assumption means the rail surface can be protected from leaf contamination when enough heat is applied to the contact. Although the key organic acids have not yet been identified, it is worth exploring a new method for prevention.

On the other hand, the high temperature has been suggested to enhance the chemical reaction between leaf organics and rail steels (14). This enhancement might lead to higher bonding strength of the leaf film generated on the rail surface. Therefore, the relationship between temperature and bonding strength should be investigated to examine the negative effect of this prevention method.

Hence, the aim of this study is to investigate the temperature effects on adhesion levels as well as the bonding strength of the leaf film using a twin disc machine.

2. Experimental details

2.1 Sample preparation

Brown sycamore leaves were collected in Sheffield between October and December in 2017. Sycamore leaves were chosen as they have been known to be one of the leaves for causing low adhesion in autumn (1–3), and they have also been used in previous studies (6,12,15,16). Based on the results of pin-on-flat tribological tests in (12), green sycamore leaves and their derivatives were excluded in this study, as they were found to show a relatively high friction coefficient (COF) compared to brown sycamore leaf derivatives. Additionally, brown leaves are a more realistic representation of the autumn.

Figure 1 shows the preparation method of leaf-related samples examined: fine brown leaf powder (LP) and black precipitation powder made with brown leaf extracts (BBP). Brown sycamore leaves were chopped in a food blender, followed by grinding procedure with a manual coffee grinder, making fine leaf powder. The leaf powder was then filtered using a 160 μm sieve (purchased from Fisher Scientific) to obtain the finest leaf powder. Relatively large pieces of leaves (leaf mulch) were used to make leaf extracts; leaf mulch was soaked in distilled water for one to two days. Using the leaf extracts and a steel plate made of R 260 rail steel, black precipitation powder was synthesised at room temperature for one to three days, followed by boiling and grinding processes. Detailed information about this synthesis can be found in (12).

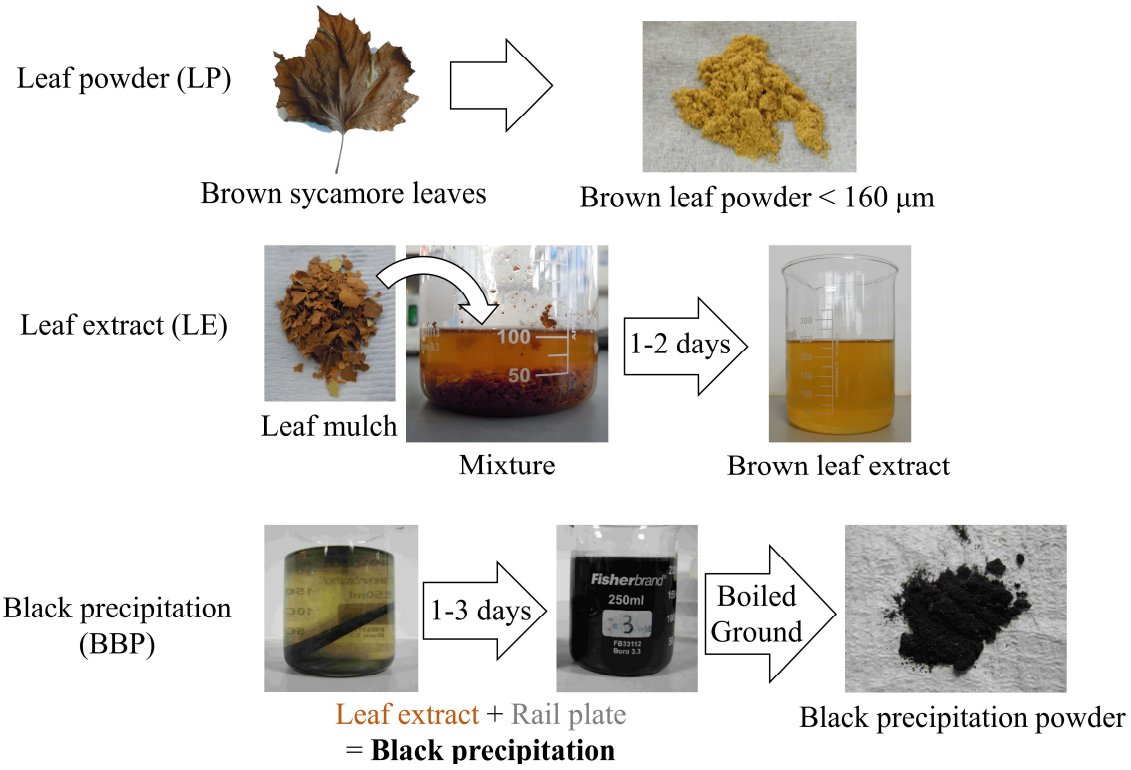

Figure 1 Preparation of leaf-related samples

In addition to the leaf-related samples, some standard materials were also examined: distilled water, engine oil (Servol 15W-40, Morris lubricant) and activated charcoal (AC), which was purchased from Sigma-Aldrich (product number: C9157, CAS number: 7440-44-0).

2.2 Friction test

2.2.1 Test equipment and Specimens

A twin disc tribology machine called SUROS (Sheffield University ROlling Sliding machine) was used to replicate a rolling-sliding contact between train wheels and rails and investigate tribological properties of the samples under such conditions. Figure 2 illustrates the schematic diagrams of the SUROS machine and 47 mm diameter disc specimens cut from rail steel (R260) and wheel steel (R8). These two discs were loaded against each other by a hydraulic pump, and they were individually driven by a Colchester Mascot lathe and an AC motor. The wheel disc was driven faster than the rail disc, replicating traction conditions between wheels and rails. The tangential contact force between the two discs was measured by a torque transducer on the shaft of the rail disc side, and traction coefficient was calculated with the tangential contact force and disc diameter. More detailed information about the test set-up of the SUROS can be found in previous studies (6,15–17).

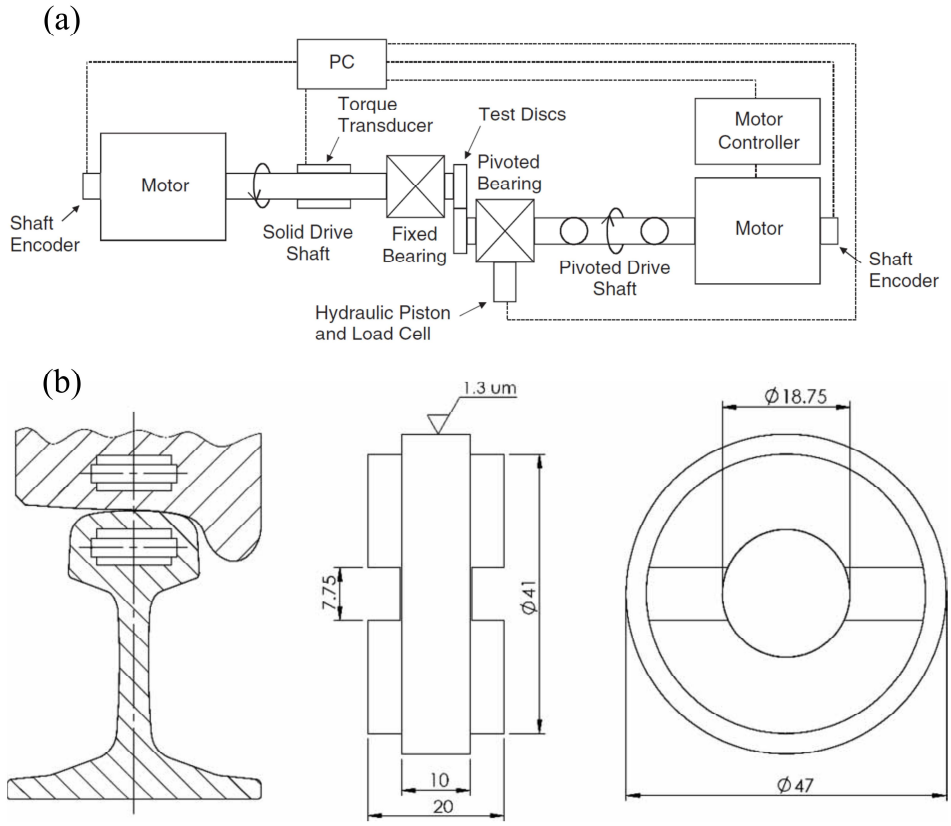

Figure 2 Schematic figures of test equipment (6)
(a) SUROS machine, (b) Disc specimens

2.2.2 Friction test procedure without pre-heating

Figure 3 shows a schematic figure of the traction curves in the SUROS tests at different slip ratios. The traction coefficient data can be divided into three phases: running-in, sample application and recovery. The traction coefficient usually showed a stabilised value during the running-in period, and then it plunged when the sample was applied. The traction maintained a low level during the sample application (approximately 20 seconds), and then it showed a recovery, back to the dry level.

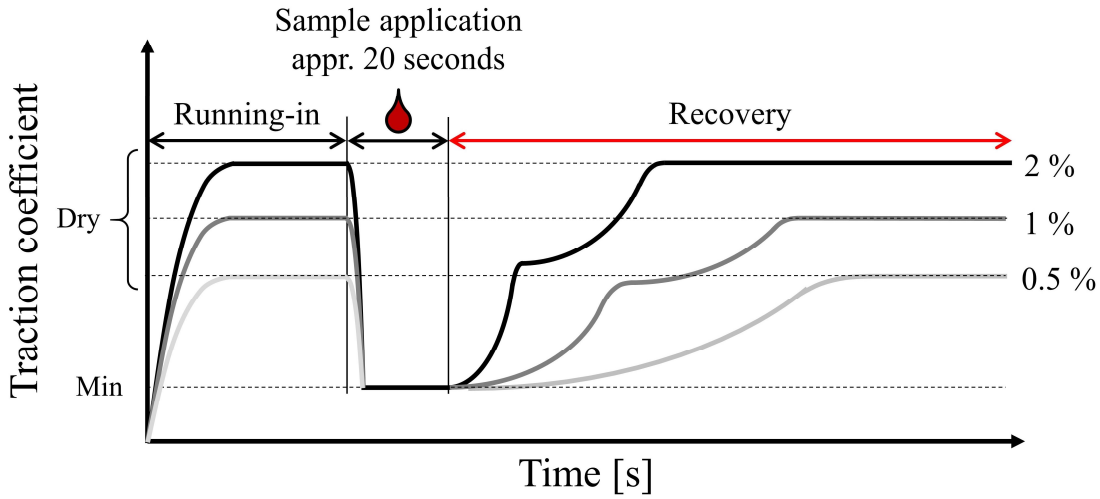

Figure 3 Schematic figure of traction curves at different slips

Figure 4 illustrates the application process of the sample suspension to the rail disc. Friction tests were carried out as follows.

1. Two discs were cleaned with acetone in an ultrasonic bath and then mounted in the machine.

2. The discs were allowed to run under dry conditions for four to five minutes until the traction coefficient stabilised (running-in).

3. The sample was then applied to the upper rail disc while measuring the traction coefficient (sample application).

4. The test was stopped after the traction coefficient had roughly recovered to the dry condition level (recovery).

5. The test was repeated three times at each slip value.

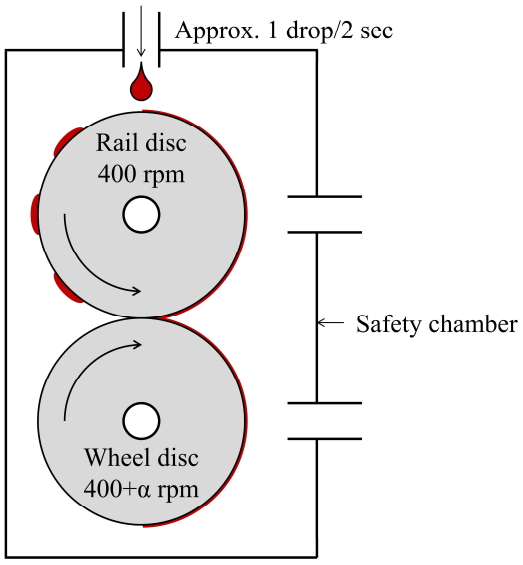

Figure 4 Schematic diagram of traction test procedure with liquid samples

Table 1 summarises the experimental conditions. The rail disc was driven at 400 rpm, which is approximately 1 m/s, but the wheel disc was driven at more than 400 rpm, depending on the slip values. Slip values were calculated following the definition in (15), and 0.5, 1 and 2 % were chosen since the contact at small slip values, which has both stick and slip region, is important in terms of vehicle dynamics (18). In the wheel/rail contact, the traction coefficient is likely to saturate at around 1-2 % slip, and the whole contact patch becomes pure-sliding in dry conditions (19,20). Hence, the friction behaviour at these small values was explored in this study.

Table 1 Experimental conditions of SUROS friction tests without pre-heating

Parameter	Value
Disc diameter [mm]	47
Average Hertzian pressure [GPa]	1.2
Speed [rpm]	400
Slip value [%]	0.5, 1, 2
Sampling frequency [Hz]	1
Sample	Distilled water, Engine oil, AC, LP, BBP
Concentration of sample suspension [wt%]	5
Application rate [drop(s)/second]	0.5
Sample amount in total [ml]	0.4-0.6 (10 drops) *1 drop for engine oil
Repetition [times]	3 *only for the test without pre-heating

AC, LP and BBP powder were applied to the disc in the form of suspensions, which are called AC suspension, LP suspension and BBP suspension, respectively. The concentration of sample suspension was fixed at five weight percent (wt%), and 0.4 to 0.6 ml of sample suspension was applied to the rail disc at approximately 1 drop/2 seconds (around 20 seconds for 10 drops). It should be noted that only 1 drop of the engine oil was applied as it showed such long-term low friction with three drops that the comparison between the other samples was difficult.

2.2.3 Friction test procedure with pre-heating

Figure 5 exhibits the pre-heating procedure, conducted only with five wt% LP suspension. In this test, both rail and wheel discs were heated up before the actual friction tests. The procedure of friction tests with pre-heating is described below.

1. Two discs were cleaned with acetone in an ultrasonic bath and then mounted in the machine.

2. The discs were tested for five to seven minutes at one of these slip values: 4, 7, 10, 15 or 20 %, depending on the target temperature.

3. The test was stopped, and the surface temperature of the rail disc was measured with a k-type thermocouple.

4. The machine was restarted and operated for one to two minutes at 0.5 or 1 % slip to stabilise the traction coefficient.

5. LP suspension was then applied to the upper rail disc.

6. The test was then stopped after the traction coefficient had roughly recovered to the dry condition level.

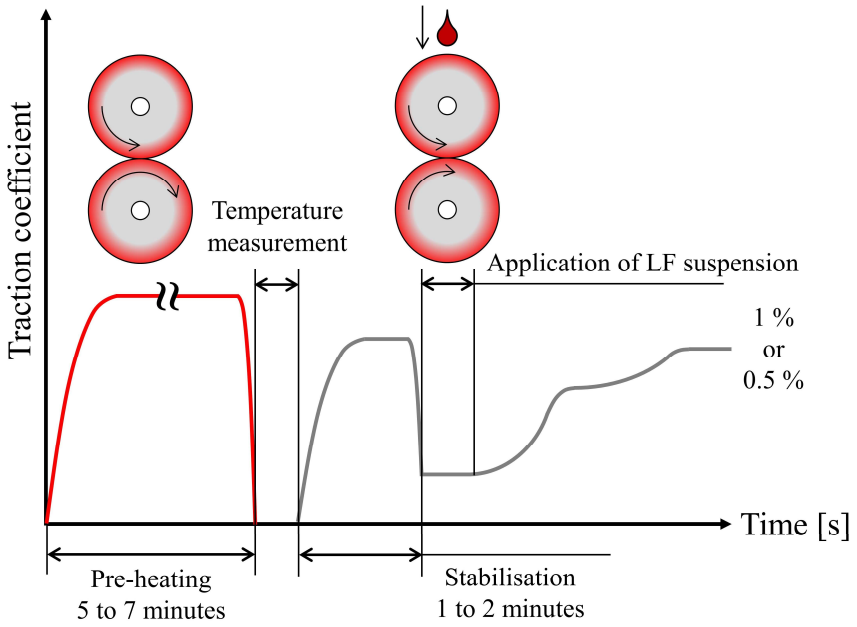

Figure 5 Test procedure with pre-heating process

The measured temperature was defined as the surface temperature, although the actual temperature during the test seems to be slightly lower than that because of the time lag between the measured point and experiment. Note that the pre-heating process uniformly raised the whole disc temperature, not only the surface. Hence, the temperature drop during the stabilisation period is believed to be not significant.

The slip value in the pre-heating process was determined considering the proportional relationship between surface temperature and slip values obtained by a thermal camera in (21). The pre-heating test at 4, 7, 10, 15 and 20 % increased the surface temperature approximately to 80, 100, 140, 180 and 200 °C, respectively. A trial experiment estimated these temperature values, and the estimated temperature roughly matched the thermal camera data in (21), although there was still an error. It should be noted that the test was conducted only once, not three times like the friction test without pre-heating.

2.2.4 Evaluation of traction coefficient

Figure 6 shows the evaluation method of the acquired traction data. Three figures were calculated from the curve: average traction coefficient of the running-in (μ_D), sample suspension (μ_L) and average recovery time (T_R). μ_D is the average value for 30 sec before the sample application commences, and μ_L is the average traction coefficient for 15 sec after the sample suspension is applied. T_R is the time when the traction coefficient reaches 0.2 after the sample suspension is applied, which is the minimum requirement for traction (2). Based on this T_R, the sliding distance SD_R was calculated following Equation 1.

$$\boldsymbol{SD_R = \alpha V T_R} \qquad \textbf{Equation 1}$$

where α stands for the slip ratio, and V does for velocity (m/s). In this test, V is approximately 1 m/s, and α is either 0.5, 1 or 2.

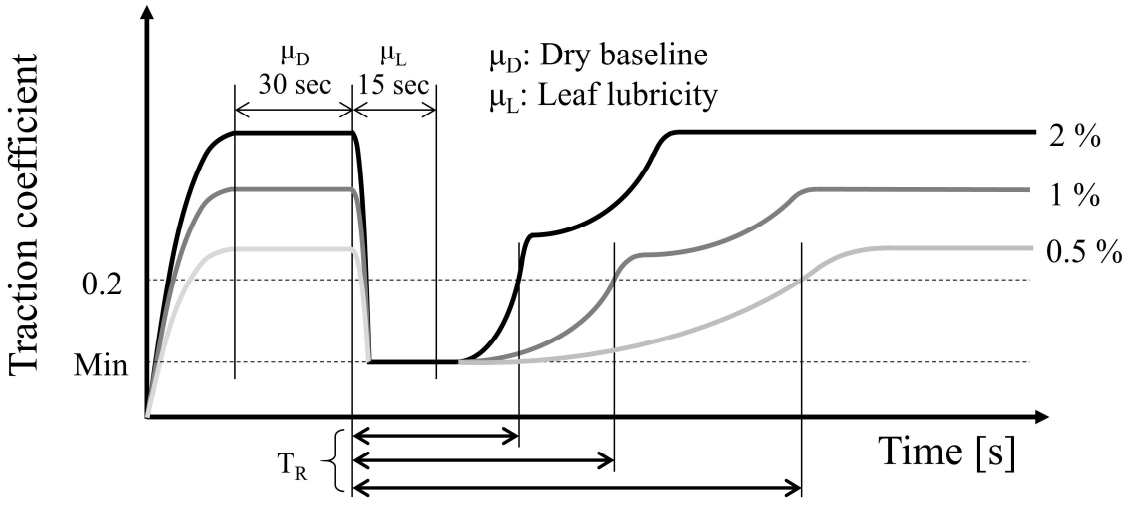

Figure 6 Definition of μ_D, μ_L and T_R

2.3 Leaf layer creation

Figure 7 shows the procedure to create leaf layers on the disc. The more detailed procedure was as follows.

1. Two discs were cleaned with acetone in an ultrasonic bath and then mounted in the machine.

2. The discs were tested for five to seven minutes at one of these slip values: 7, 12 or 20 %.

3. The test was stopped, and the surface temperature of the rail disc was measured with a k-type thermocouple.

4. The machine was restarted and operated for one to two minutes at 1 % slip to stabilise the traction coefficient.

5. 1 ml of 10 wt% LP suspension was applied to the rail disc for approximately 30 to 40 seconds.

6. The operation was stopped as soon as the application finished.

The surface temperature of the disc was raised before the leaf film creation. As a reference, a leaf film was also created at room temperature without pre-heating. The purpose of this pre-heating process is to examine the hypotheses of the bonding mechanism developed in (14): "sub- or supercritical water", "catalyst function of iron oxides" and "cellulose or lignin adhesives".

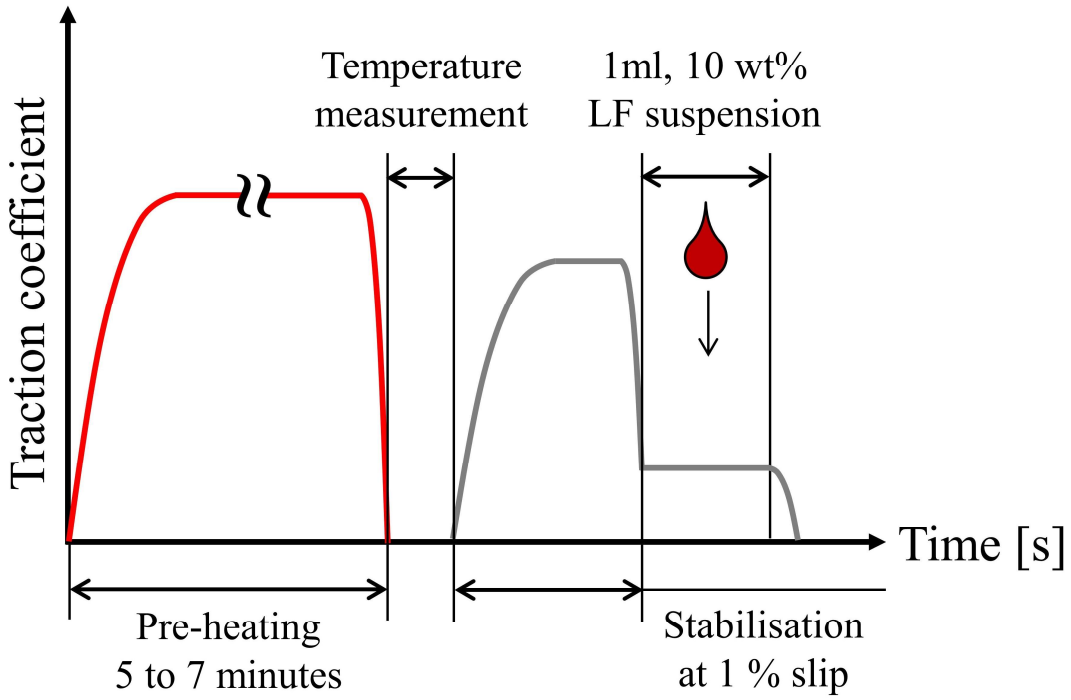

Figure 7 Leaf film creation process

2.4 Characterisation

The created black leaf film was analysed mechanically and chemically: Scratch Test, Laser Raman spectroscopy and Fourier transform infrared spectroscopy.

2.4.1 Scratch test

Scratch testing is a common technique used to mechanically estimate the bonding energy (adhesion energy) between substrates and films or coatings on them, e.g. resistant coatings (22). Figure 8 illustrates the schematic figures of the conducted scratch tests. In this study, a simple scratch test was conducted at a constant load with a micro Rockwell stylus which has a 200 µm diameter diamond ball. Before scratching, half of the leaf film on the disc was removed by sandpaper, exposing a bare steel surface as shown in Figure 8 (a). A Rockwell indenter was then pressed with 20 N, and it pulled across the surface at 0.05 mm/s, ploughing the disc surface and breaking the leaf film as shown in Figure 8 (b). After scratching, the width of the scratch traces was measured by an optical microscope (Figure 8 (c)). The bonding energy can be estimated by calculating the area while the leaf film was being destroyed by the indenter, as shown in Figure 8 (d). Finally, the bonding energy per unit area (Jm^{-2}) was calculated with the estimated scratch length in Figure 8 (d), following Equation 2 (23–25).

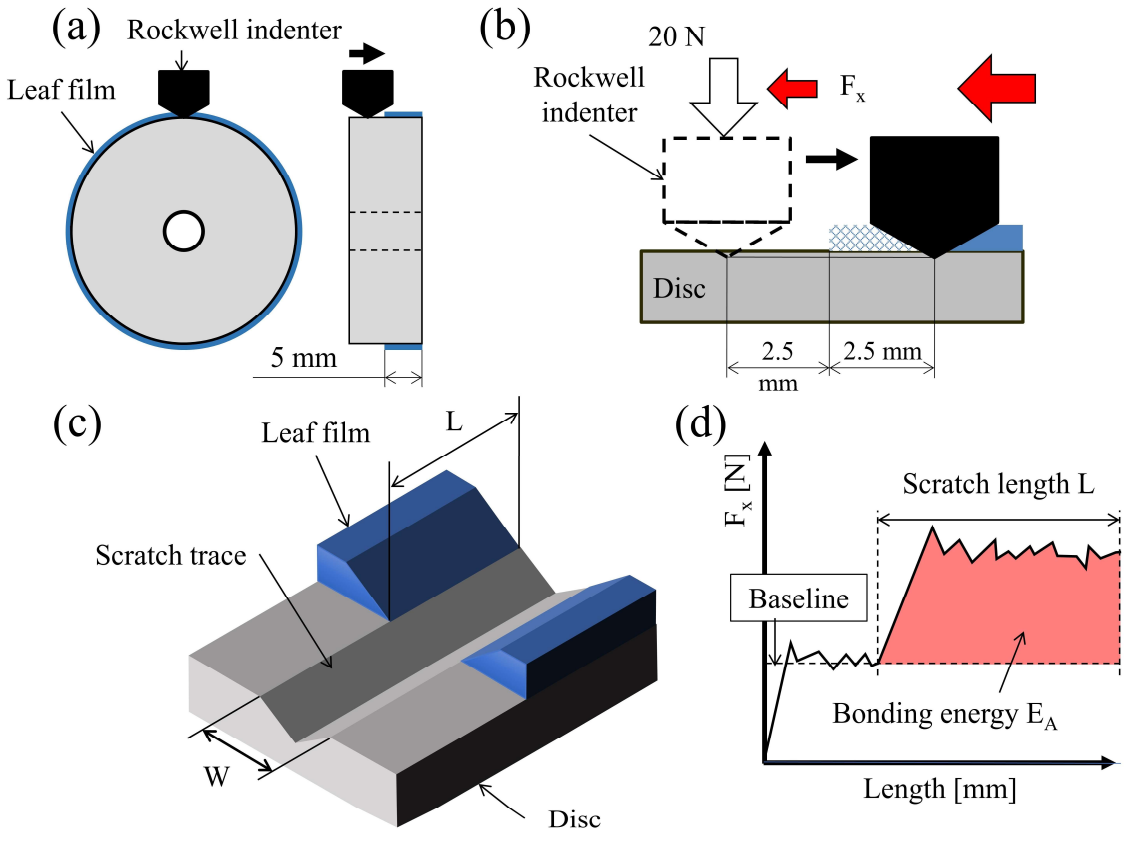

Figure 8 Schematic figures of scratch test
(a) Removal of leaf film, (b) Scratch test procedure, (c) Valuables, (d) Bonding energy calculation

$$\frac{E_A}{A} = \frac{E_A}{W \cdot L}$$ **Equation 2**

The main aim of the scratch tests was to estimate the approximate bonding energy of leaf films and compare the estimated bond strength of the films created at different temperature. Since the created leaf films were non-uniform and unsmooth, measurements of a critical load were not attempted, although that is more common in scratch tests (26).

2.4.2 Laser Raman Spectroscopy (RS)

A Renishaw inVia Raman Microscope was used for RS analysis with the black leaf film formed on the disc. The wavelength of the laser was 514.5 nm (green), and the original laser power was set as 20 mW. In all experiments, the objective lens x50 was used, and the spot size was approximately five μm in diameter. The spectrum was acquired between 50 and 4000 cm^{-1} with the exposure time of 20 seconds and five-time accumulation, reducing the laser power to 10 % (approximately two mW). A baseline of the acquired spectrum was subtracted, and the noise on the spectrum was removed with WiRE software, making the spectrum flat and smooth. The main aims of the RS analysis are to confirm the formation of graphite-like carbon in the leaf film and to study the effects of experimental conditions on the property of the leaf film.

2.4.3 Fourier Transform Infrared Spectroscopy (FT-IR)

A Bruker ALPHA Platinum-ATR was used, and the leaf films created at room temperature, 106, 140 and 227 °C were analysed. The absorption band between 400 and 4000 cm^{-1}, was mainly analysed, scanning 16 times with the resolution of 4 cm^{-1}. The fingerprint region between 600 and 1500 cm^{-1} was also analysed; however, the interpretation could be incorrect as this region usually shows complex absorption patterns. The equipment uses a diamond stage; hence, the spectra had a noise between 1900 and 2200 cm^{-1}, and the interpretation in this region was not attempted. The objective of this FT-IR analysis is to study the effects of experimental conditions on the chemical bonds in the leaf film by comparing the spectrums.

3. Results and Discussion

3.1 Twin disc friction tests

3.1.1 Friction test without preheating

Figure 9 exhibits an example of the friction test result, which was taken with the LP suspension at 2 % slip without the pre-heating process. The friction behaviour showed the pattern described in 2.2.4: constant traction coefficient in dry conditions, followed by the sudden decrease due to the sample application, and then the recovery. As can be seen, μ_D represents the baseline traction coefficient in dry conditions, and μ_L shows the traction coefficient due to the sample suspension.

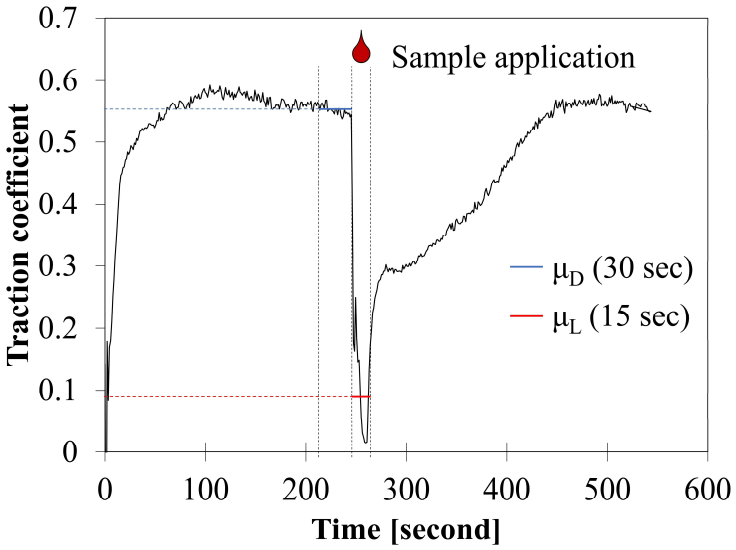

Figure 9 Example of the friction test: 5 wt% LP suspension at 2 % slip without pre-heating

Figure 10 (a) shows an example of raw traction data at 0.5, 1 and 2 % taken with the distilled water. At all the slips values, the traction coefficient dropped after the water application, and then the recovery was seen. The recovery behaviour depends on the slip value; the gradual recovery was seen at 0.5 %, but there was a relatively quick recovery at 2 %. Figure 10 (b) shows the creep curves of the average traction coefficient: μ_D and μ_L. μ_L was around 0.2 at all slip values, showing a good agreement with the previous study apart from 0.5 % slip (5).

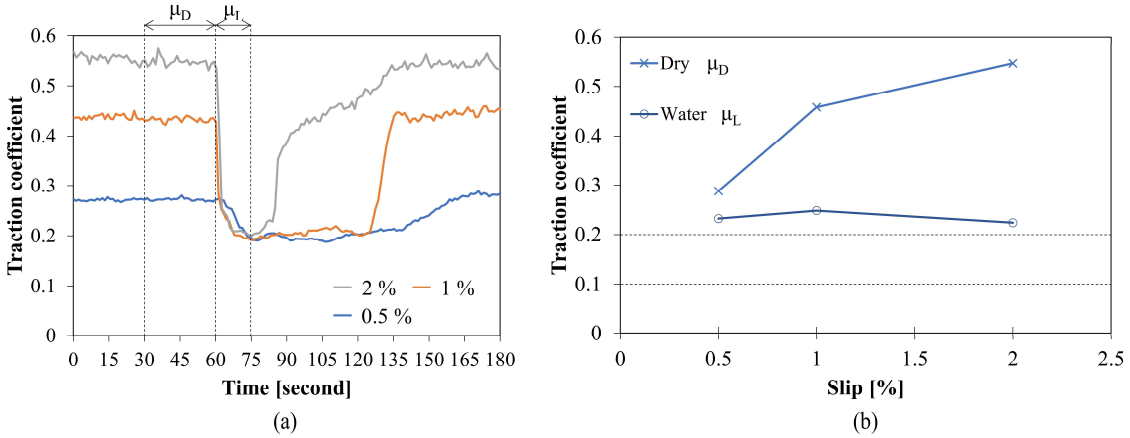

Figure 10 Traction behaviour of distilled water
(a) Comparison of typical traction data at 0.5, 1 and 2 % slip, (b) Creep curves

Figure 11 (a) shows an example of the frictional behaviour of the engine oil, and Figure 11 (b) exhibits the creep curves of μ_D and μ_L. There was no clear recovery region, and μ_L was around 0.1 at all the slip values. As expected, the engine oil showed a very stable and low traction coefficient, and the higher slip did not seem to affect its performance.

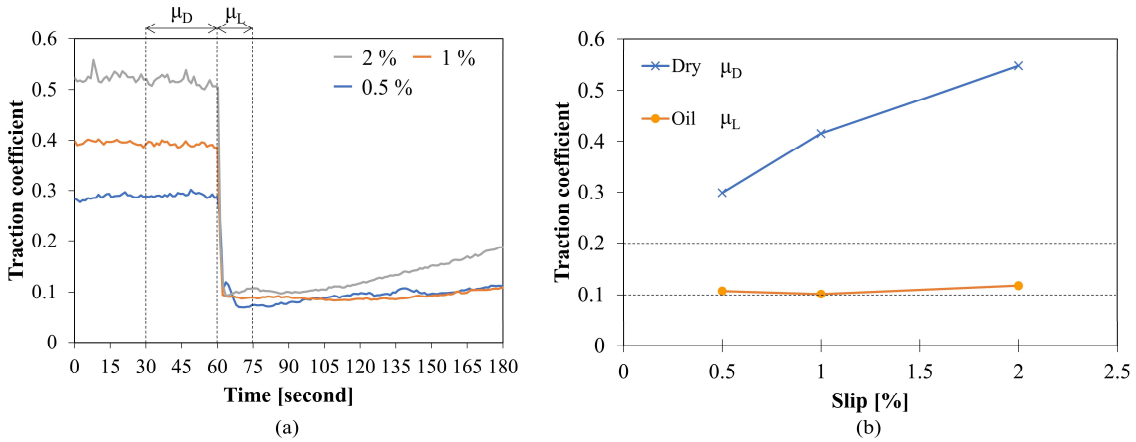

Figure 11 Traction behaviour of engine oil
(a) Comparison of traction data at 0.5, 1 and 2 % slip, (b) Creep curves

Figure 12 illustrates the frictional behaviour and creep curves of the LP suspension. LP suspension was found to show the low traction coefficient at all slip values. In particular, μ_L reached almost the detection limit at 0.5 %, and it still kept the low level at 1 and 2 % slip. As shown in Figure 12 (b), μ_L at 0.5 and 1 % slip met neither the traction requirement 0.2 nor braking requirement 0.1 (2), and μ_L at 2 % slip did not reach 0.2. Moreover, μ_L at all slip values was lower or at the same level as the engine oil, showing a good agreement with the result in (12). On the other hand, the recovery after the sample application became more distinct as the slip increased. It should be noted that the LP suspension became black immediately after it was applied to the disc surface, indicating that the chemical reaction between leaf organics and iron had happened.

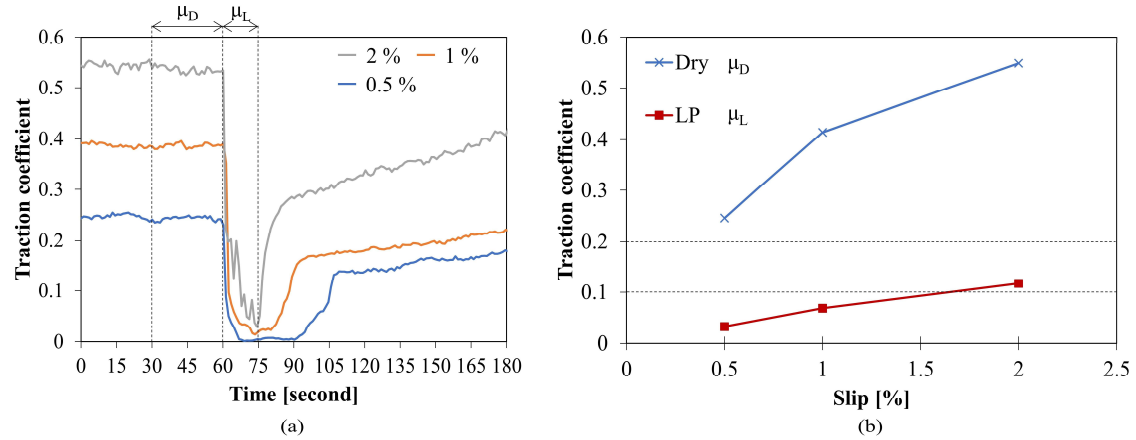

Figure 12 Traction behaviour of LP suspension
(a) Comparison of traction data at 0.5, 1 and 2 % slip, (b) Creep curves

Figure 13 depicts the frictional behaviour and creep curves of BBP suspension. The frictional behaviour was analogous to the LP suspension; low traction coefficient and more noticeable recovery as the slip value increased. μ_L was lower than 0.1 at 0.5 and 1 % slip, and it met the braking requirement but failed to reach 0.2 at 2 % slip, as shown in Figure 13 (b).

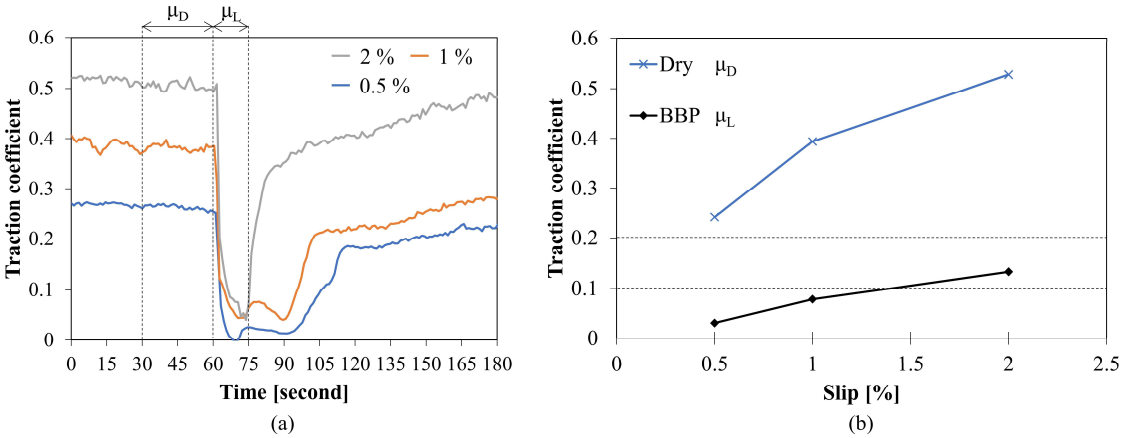

Figure 13 Traction behaviour of BBP suspension
(a) Comparison of traction data at 0.5, 1 and 2 % slip, (b) Creep curves

Figure 14 illustrates the comparison of traction data and creep curves of AC suspension. Unlike the LP and BBP suspension, the AC suspension showed a low and constant traction coefficient between 0.1 and 0.2, and there was no distinct initial recovery region. This consistently low traction shows that the black material formed in the LP and BBP tests had different tribological property from the AC.

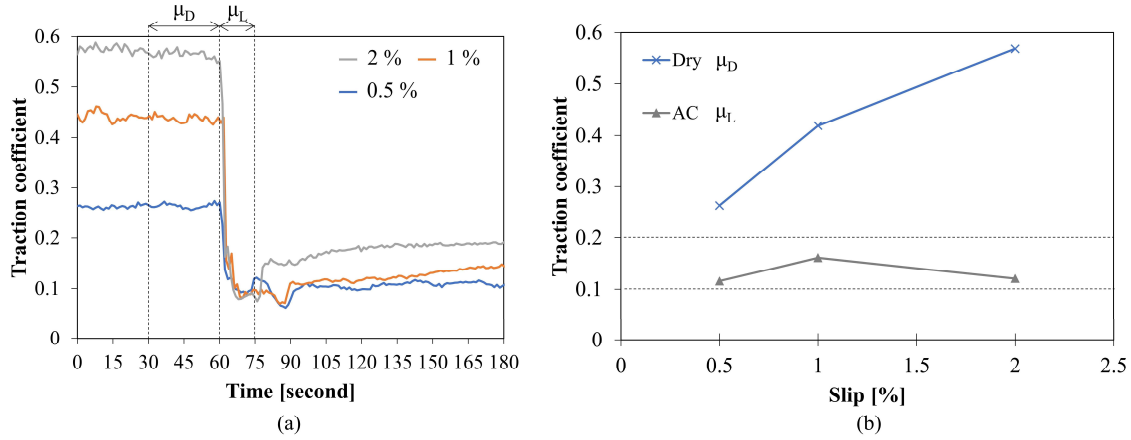

Figure 14 Traction behaviour of AC suspension
(a) Comparison of traction data at 0.5, 1 and 2 % slip, (b) Creep curves

Figure 15 shows the sliding distance, which can reach 0.2 after the sample application. The error bar shows a standard deviation value. Figure 15 (a) shows the SD_R of AC and engine oil. It should be noted that the distilled water was unable to be evaluated since its minimum traction coefficient was almost 0.2 or higher. The AC 5 wt% suspension showed a similar SD_R value around 5 to 6 m at 1 and 2 % slip. The engine oil showed almost the same SD_R value around 2 m at all the slip values. This relatively constant level of SD_R means that the recovery depends on the sliding distance rather than the slip ratio; sliding surface helps remove the AC and engine oil.

Figure 15 (b) shows the SD_R of BBP and LP. In comparison with the AC and engine oil, BBP and LP were found to have less SD_R, less than 1 m. BBP had the same SD_R at all slips around 0.4 m like the engine oil; however, LP had less SD_R at 2 % slip, around 0.4 m, than the SD_R at 0.5 and 1 % slips. This different trend in the SD_R means that other factors might be able to contribute to the recovery in the case of LP suspension, not simply depending on the sliding distance.

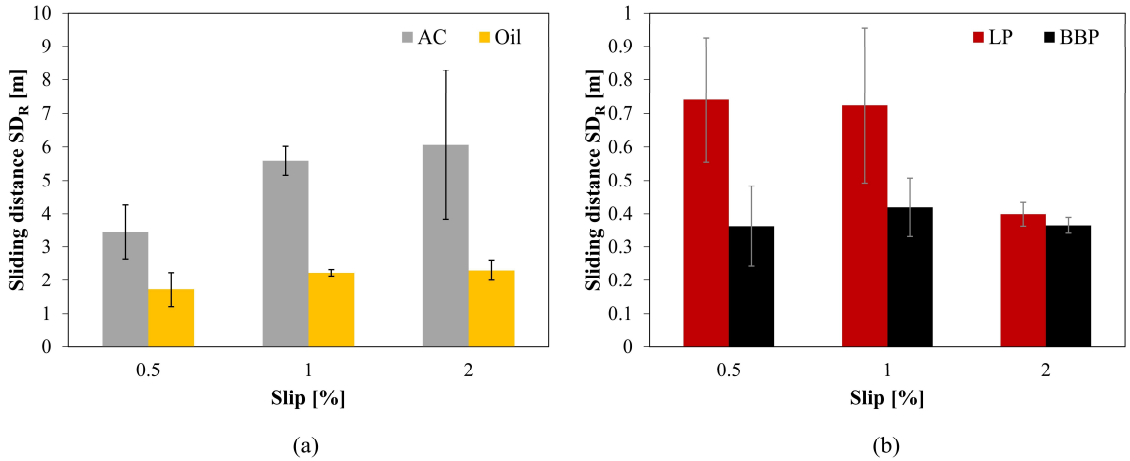

Figure 15 Comparison of the SD_R for each sample
(a) AC and engine oil, (b) LP and BBP

Potential differences related to a higher slip value could be an increase in surface temperature during the running-in period. The surface temperature was measured by the method presented in 2.2.3 after five minutes operation at 0.5, 1 and 2 % slip in dry conditions, as summarised in Table 2. The surface temperature was confirmed to increase as the slip value increased, and the difference between 0.5 and 2 % slip was around 20 °C. Unlike BBP and LP, SD_R of the engine oil was not affected by the temperature change, although the viscosity of oil strongly depends on temperature. One possible explanation is that the lubrication regime in this test was either boundary or mixed, and the viscosity change had little effect on the lubrication. Since the change in the surface temperature was found, the effect of surface temperature on traction coefficient was investigated with pre-heating process.

Table 2 Surface temperature after the operation at 0.5, 1 and 2 % slip

Slip value [%]	Surface temperature [°C]
0.5	44.3 ±2.8
1	51.8 ±1.5
2	63.7 ±0.6

3.1.2 Friction test with pre-heating

Figure 16 depicts the traction behaviour of LP suspension at 0.5% slip, which was taken at various temperatures with the pre-heating process. Figure 16 (a) is the comparison of the

acquired traction data at 42, 106, 180 and 211 °C (zoomed-in view). As the temperature increased, the traction coefficient μ_L in the sample application region increased, and only a subtle drop was observed at 211 °C. Moreover, the recovery region started much earlier at 106 °C than 42 °C, and no significant drop was observed at 180 and 211 °C. Figure 16 (b) shows the relationship between the surface temperature and traction coefficient μ_L, with μ_D as a reference value. The proportional relationship was observed, and the traction requirement 0.2 would be achievable at around 240 °C if this linear trend continues. In contrast, μ_D showed a slight increase as the temperature increased, meaning that the temperature had fewer effects on traction in dry conditions.

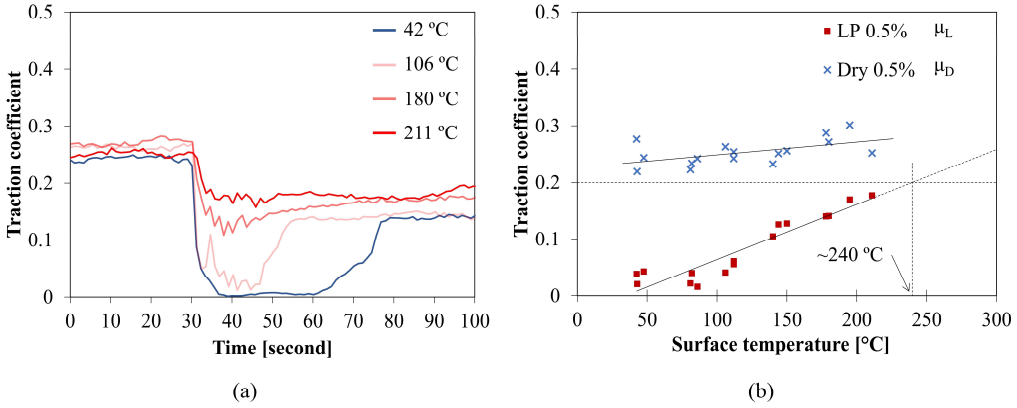

Figure 16 Traction behaviour of LP suspension at 0.5 % slip with pre-heating process
(a) Comparison of traction data, (b) Relationship between temperature and traction coefficient

Figure 17 exhibits the traction behaviour of LP suspension at 1 % slip and various temperatures. In the same manner as the data at 0.5 % slip, μ_L became larger as the temperature increased. Due to this larger μ_L, the recovery region was hardly seen at 159 and 196 °C. These changes in μ_L and μ_D led to the larger traction coefficient at the higher temperature, which probably reaches 0.2 at around 240 °C. In contrast, μ_D decreased as the temperature increased, reflecting the negative effect of friction heat on the friction coefficient (18).

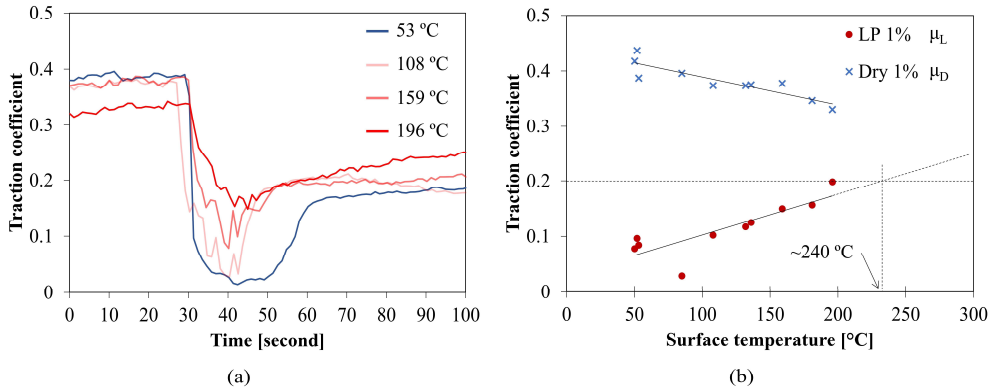

Figure 17 Traction behaviour of LP suspension at 1 % slip with pre-heating process
(a) Comparison of traction data, (b) Relationship between temperature and traction coefficient

3.2 Analysis of created leaf layer

3.2.1 Visual inspection

Figure 18 depicts photographs of the created leaf layers at various temperatures: room temperature, 106 °C, 140 °C and 227 °C. The black material was formed on both the wheel and rail discs at room temperature. However, the black leaf film was created only on the wheel disc at 106, 140 and 227 °C, and the leaf film at 227 °C was patchy. This partially formed film at high temperature shows that thermal energy does not seem to enhance the chemical reaction and help the formation of leaf films. Note that the leaf film at room temperature was pretty powder-like, while the other black films seemed to be similar to the actual leaf films on a rail.

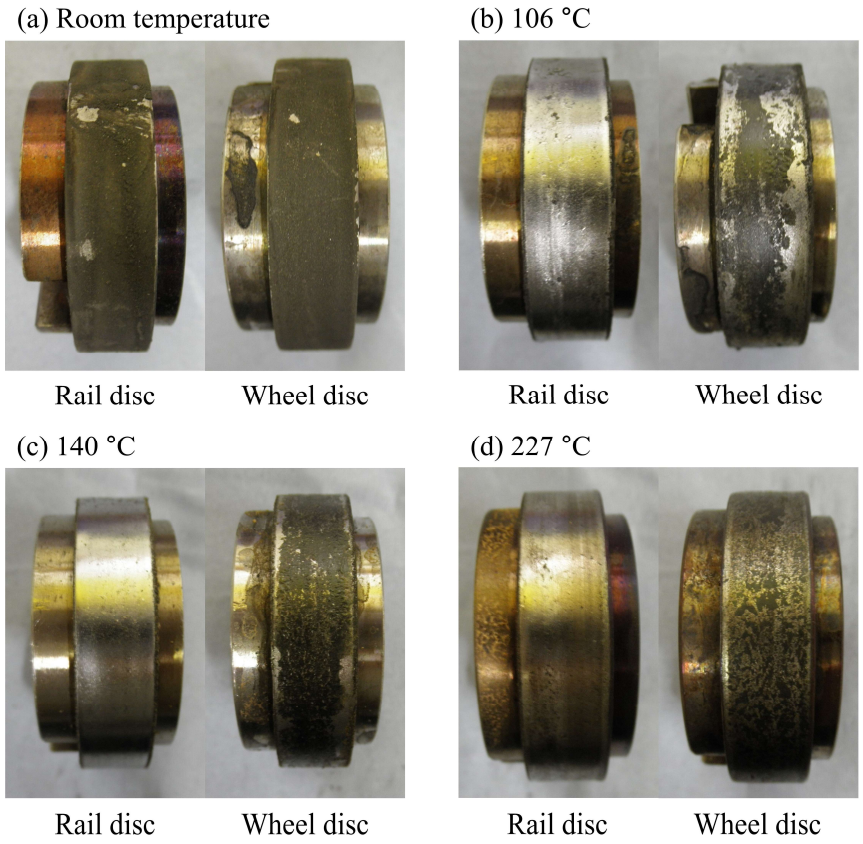

Figure 18 Created leaf films on SUROS discs at various temperature
Created at: (a) Room temperature, (b) 106 °C, (c) 140 °C, (d) 227 °C

3.2.2 Scratch tests

Figure 19 exhibits an example of the scratch test result conducted for the leaf film created at 106 °C. The mean value of the lateral force was calculated by averaging the lateral force in the exposed surface region, and the bonding energy was then estimated. It was found that the baseline showed a less constant level than expected, and this relatively large error, around 10 %, could be caused by the rougher surface due to the prior removal of leaf films by sandpaper.

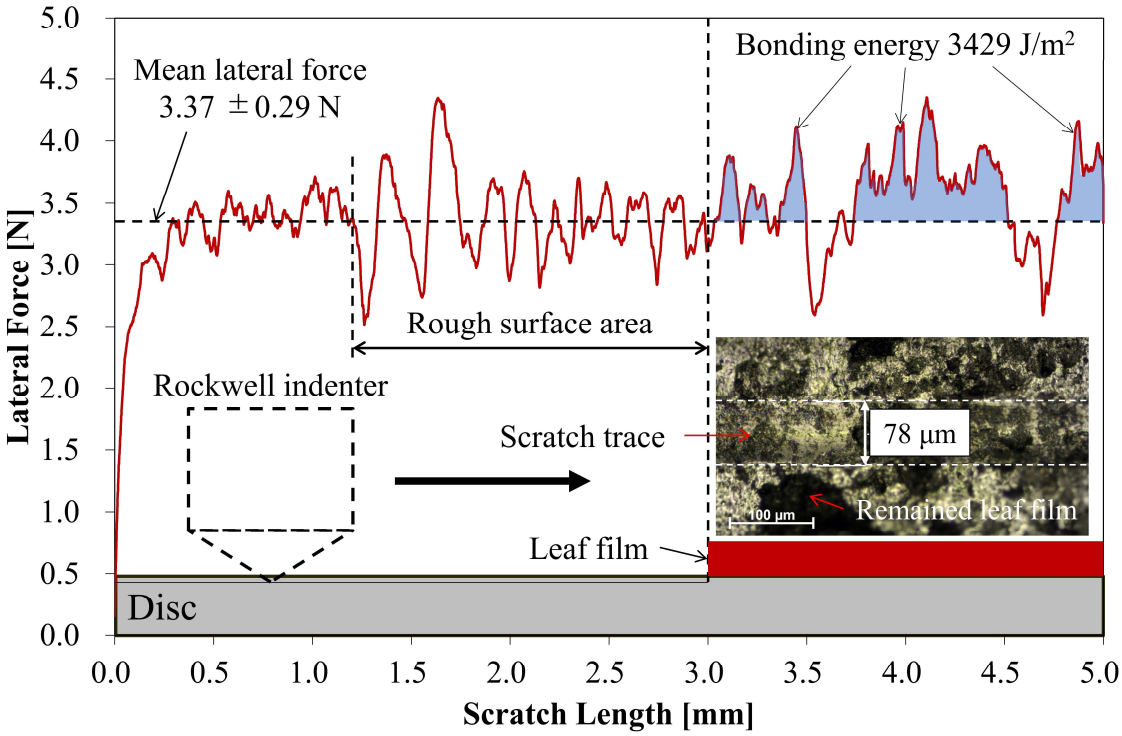

Figure 19 Example of scratch test result: leaf film created at 106 °C

Figure 20 shows the comparison of the bonding energy of the created leaf films at different temperatures. Note that the leaf film created at 227 °C was unable to be evaluated since there was not enough leaf film left. No clear difference in the bonding energy was found due to the large error, but the decreasing trend still can be seen between 106 and 140 °C. Since the leaf film became patchy at 227 °C, the high temperature is likely to weaken the bonding strength of leaf films as well as prevent the leaf film formation.

Furthermore, all the leaf films were easily removed by nail-scratching, showing that they did not tightly adhere to the rail substrate. This small energy indicates that the high temperature is unlikely to increase the bonding strength. Although there could be a better methodology to generate well-adhered leaf films, the application of heat energy was shown to be a potential prevention and mitigation method without the significant negative impact on leaf film bonding.

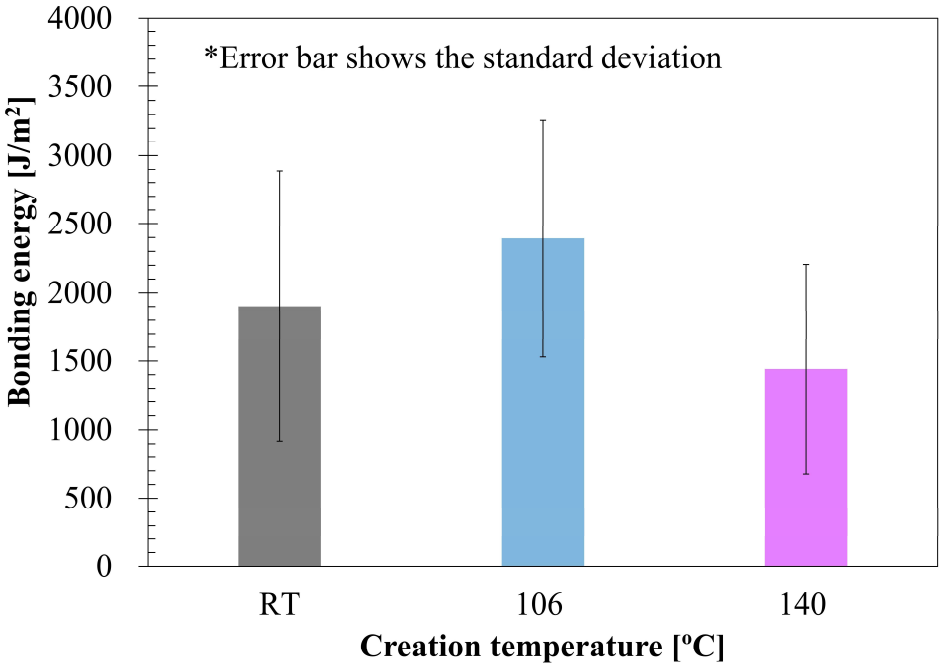

Figure 20 Comparison of bonding energy of leaf films generated at different temperatures

3.2.3 Laser Raman Spectroscopy

Figure 21 shows the comparison between the acquired Raman spectra of the leaf films created at different temperatures, and Table 3 shows the detected Raman shifts and their assignments. The created leaf films were found to contain amorphous carbon, which shows peaks around 1330 cm^{-1} (D band: shoulder) and 1575 cm^{-1} (G band). The intensity ratio of the D band and G band (I_D/I_G) was calculated, and it was 0.57, 0.59 and 0.65 for the leaf films at room temperature, 106 and 140 °C, respectively. These low ratios show that the leaf films have partially-graphitised carbon on their surfaces (27), and it should be the main cause of low adhesion in friction tests. Similar Raman spectra have been detected in black precipitate synthesised with leaf extracts and rail steel in (12). Hence, this black material on the leaf films seems to be the same as the artificial black precipitate.

It was also found that the peaks of iron oxides became sharper as the temperature increased. In particular, sharp peaks can be seen in the leaf film created at 227 °C. This result might indicate that high temperature prevents leaf powder from reacting with rail steel due to the quick evaporation and decomposition of organic acids, which seem to trigger the chemical reaction (12). On the other hand, the black material was still formed at high temperature. Hence, further work needs to be done to clarify the relationship between temperature and chemical reaction.

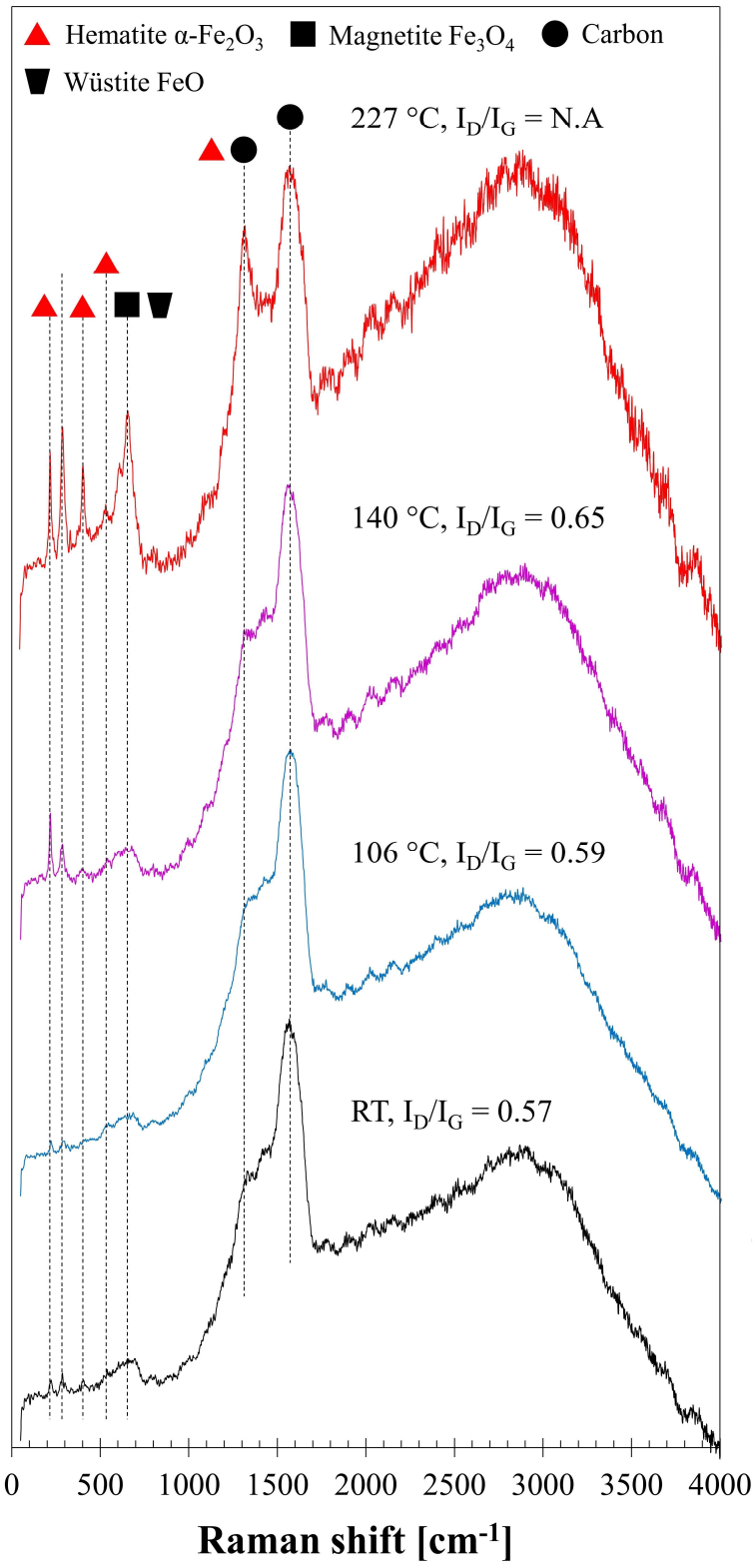

Figure 21 Raman spectra of the created leaf films at different temperatures
*** RT means room temperature**

Table 3 Raman shifts and assignments of the created leaf films

Room temperature [cm^{-1}]	106 °C [cm^{-1}]	140 °C [cm^{-1}]	227 °C [cm^{-1}]	Assignment	Reference	
222 m	220 m	218 m	222	α-Fe_2O_3	226.7	(28)
287 m	288 m	284 m	292	α-Fe_2O_3	292.5 299.3	(28)
-	(403)	(399)	407	α-Fe_2O_3	410.9	(28,29)
-	-	-	606	α-Fe_2O_3	611.9	(28)
-	-	-	661	FeO Fe_3O_4	652 662.7	(28) (29)
1330	1330	1330	1316 s	Amorphous carbon α-Fe_2O_3	1355 1320	(28–30)
1571 s	1575 s	1572 s	1576 s	Amorphous carbon Sugar-derived carbon	1575 1580	(30) (31)

*1 m and s means medium and strong, respectively

3.2.4 Fourier Transform Infrared Spectroscopy

Figure 22 illustrates the comparison of the acquired FT-IR spectra. As a reference, raw brown leaf powder was also analysed. Four samples showed the very similar absorption pattern to brown leaf powder, exhibiting that the created leaf films mainly consisted of bulk leaves. The double absorptions around 1400 and 1600 cm^{-1}, which are seen in the black precipitate as a characteristic feature (12), cannot be seen in the acquired spectra. This result suggests that the chemical reaction occurs only on the surface, forming a graphite-like carbon layer on top of the leaf film.

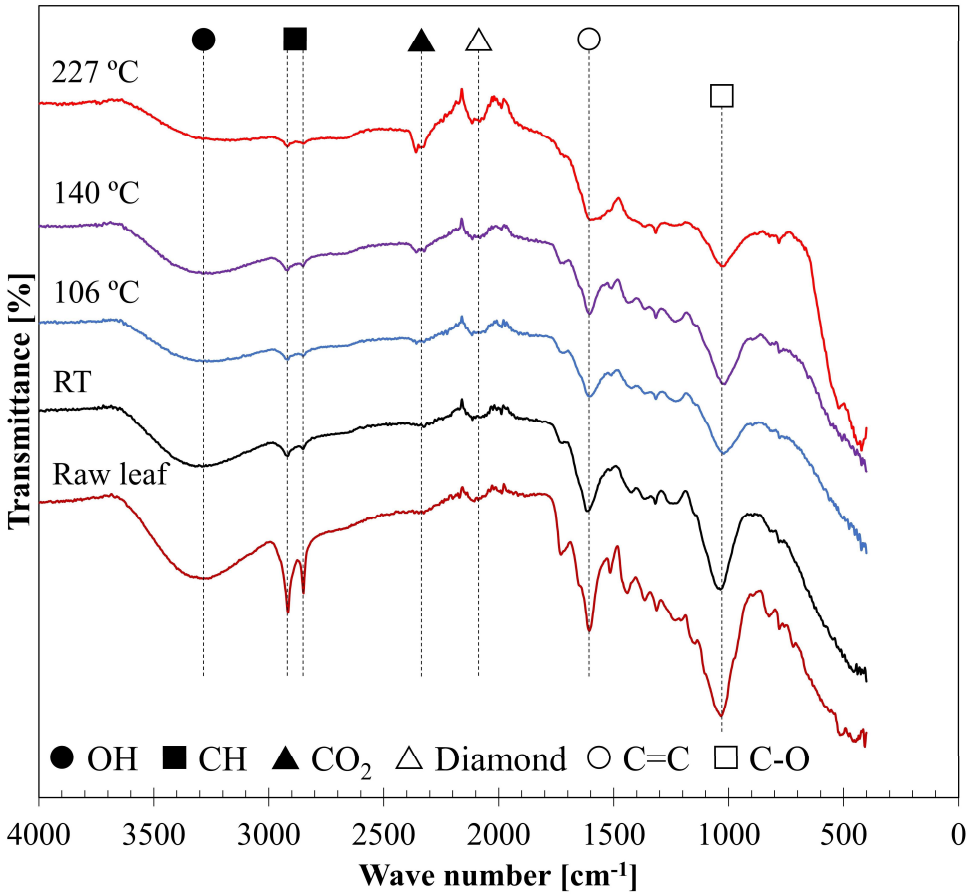

Figure 22 Comparison of FT-IR spectra
*** RT means room temperature**

Table 4 shows the assignments of the absorption bands. All the acquired bands belonged to typical organic bonds, such as C-H and C-O, and no significant difference was seen in the peak positions. Therefore, the heat energy was found to have less effect on the chemical composition of leaf films.

Table 4 Assignment of the detected infrared bands

Assignment	Leaf powder [cm^{-1}]	Room temperature [cm^{-1}]	106 °C [cm^{-1}]	140 °C [cm^{-1}]	227 °C [cm^{-1}]	Reference
OH stretch	3263	3290	3269	3244	-	(32)
CH stretch	2916 2849	2917 2851	2916 2851	2917 2851	2919 2849	(32)
C=C (Aromatic rings)	1606	1612	1605	1604	1600	(32,33)
CO stretch	1032	1035	1021	1016	1022	(32,33)

4. Discussion

4.1 Mechanism of traction improvement

The series of test with pre-heating process using LP suspension found that the surface temperature has an influence on the improvement of traction coefficients, showing the proportional relationship between the surface temperature and traction coefficient μ_L. The traction coefficient requirement, 0.2, would be achievable at approximately 240 °C, given that the linear relationship continues. This improvement at small slip values, 0.5 and 1 %, is very important for the actual train operation since it would be able to mitigate the low adhesion, not relying on mechanical methods, such as sand particle and wheel slipping, which lead to the damages of wheels and rails.

Three potential reasons for this traction improvement are listed as follows: water evaporation due to the high surface temperature, decomposition of key organic acids and mechanical deterioration of leaves as shown in Figure 23. In this test, the sample suspension was dropped to the upper rail disc running at 400 rpm. Until the stuck sample suspension on the disc reaches the contact point, the water could be evaporated to some extent, and the dried LP is more likely to be present. Dry leaves have been reported to have higher traction coefficient than wet leaves (5); thus, the loss of water could be responsible for this improvement. Additionally, the key organic acids of leaves, which are dissolved into the water, could be decomposed by the heat energy. The patchy leaf film at 227 °C in Figure 18 supports this idea, as well as the downward trend of the bonding energy in Figure 20. Moreover, the high temperature might change the mechanical properties of the leaf; the heat can make the leaf powder more fragile. The brittle leaf powder could be unable to support the load, and the leaf powder is likely to fail to prevent the metal-metal contact between two discs, being expelled from the contact area. Hemicellulose and lignin have been reported to decompose as a result of pyrolysis at 220-315 °C and 100-900 °C, respectively (34). This information supports the idea of mechanical deterioration of leaves well. Another hypothesis is that lower water viscosity could form a thinner water film between the discs, leading to higher traction (35,36). However, this hypothesis is unlikely since the lubrication regime in this test seems to be boundary or mixed, in which water is not likely to form a film.

The pre-heating method used in this study must have involved in changes of the surface condition as well, such as an increase in the surface roughness and excessive oxidative wear. These changes are likely to affect the traction coefficient along with high temperature, and the traction improvement could be the result of the mixed effect of them. In the case of graphite, rougher friction surface (13.39 μm in Ra) was reported to lower the friction coefficient than smoother surface (37). Hence, the change in surface roughness could have a limited effect on the traction improvement in the case of LP suspension. On the other hand, the effect of wear debris as a result of the pre-heating process is not clear, especially, in combination with leaf powder. So far, it is still unclear which factor is more responsible for the traction improvement seen in this study, although the high temperature seems to be more effective considering the linear relationship seen in Figure 16 and Figure 17. Another method for the pre-heating process should be used to separate the heat effect and wear debris effect, such as pre-heating in an oven and pre-heating by an induction heater. This examination will be carried out in the future.

To sum up, it was found that the high temperature has a positive effect on traction improvement, showing the direction of a new prevention and mitigation method against leaf contamination.

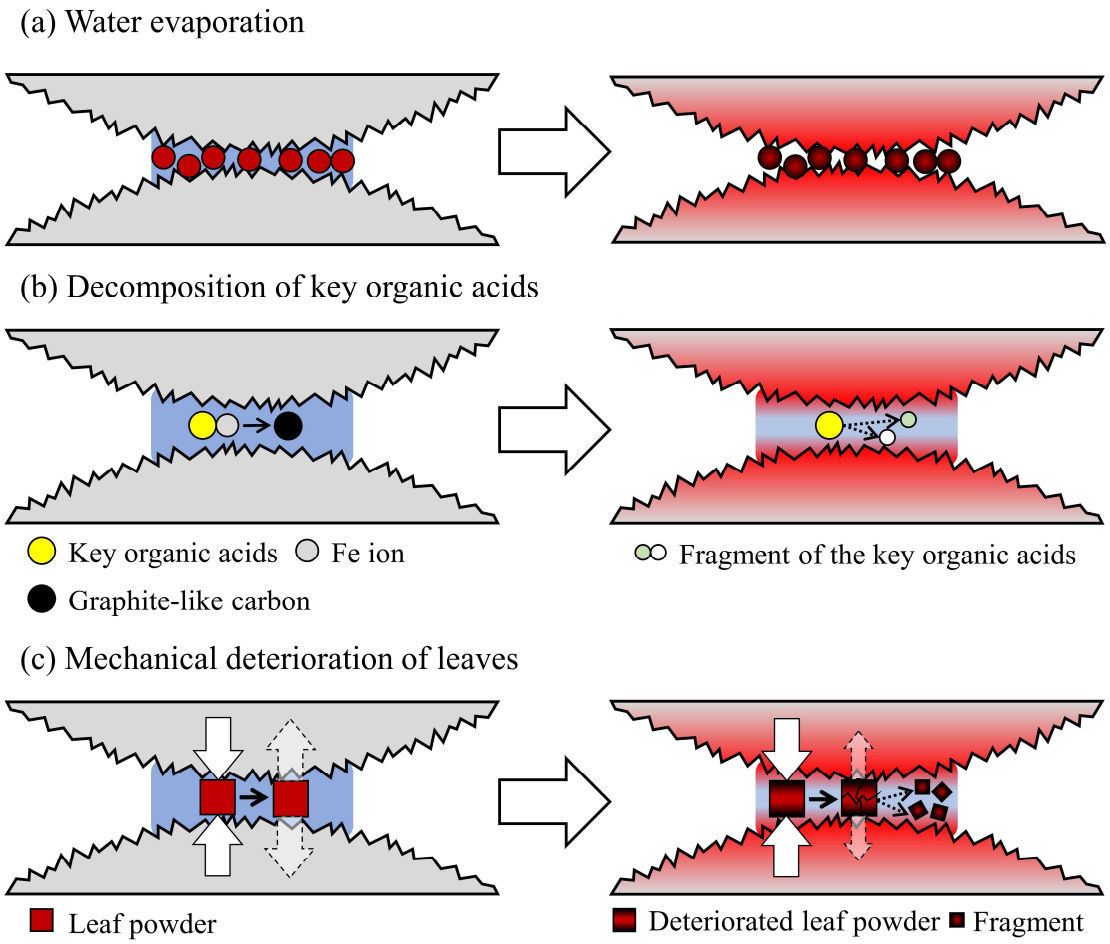

Figure 23 Three potential mechanisms of the traction improvement

4.2 Low adhesion mechanism in rolling-sliding contact

Figure 24 shows the low adhesion mechanism proposed in this study. Figure 24 (a) shows the first step of the mechanism; key organic acids are discharged into the water around the leaves by the passing-wheels, as suggested in the previous study (12). As the RS analysis showed, a soft graphite-like carbon layer is then formed on top of the pieces of leaf thanks to the chemical reaction (Figure 24 (b)). When the following wheel rolls over the blackened leaves, the wheel is likely to slip due to the reduced friction level. The slipping wheel helps pick up the soft graphite-like carbon layer, spreading the low adhesion according to the result presented in 3.2 (Figure 24 (c)). After passing wheels remove the superficial black layer, the chemical reaction might re-occur due to the freshly exposed leaf surface, re-forming the graphite-like carbon layer.

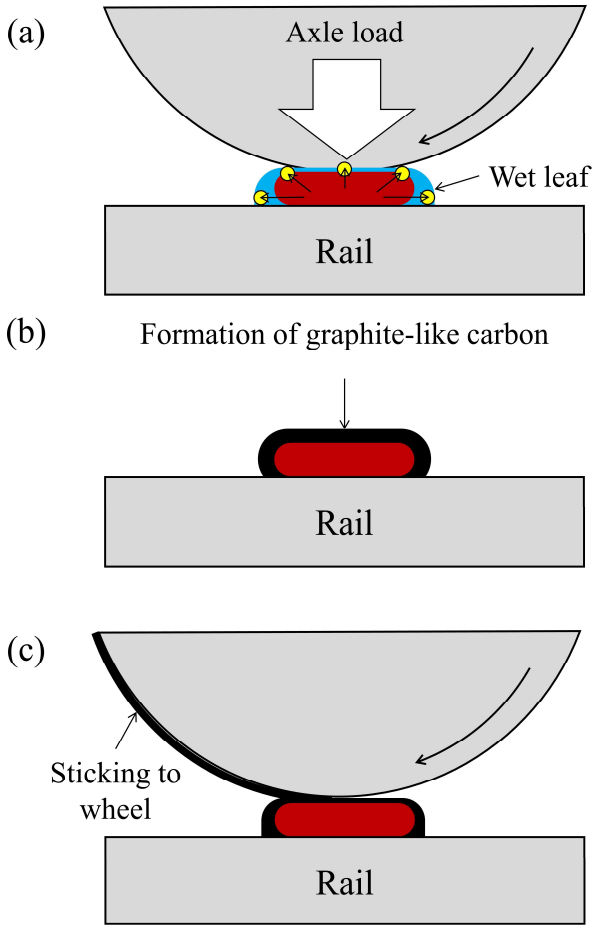

Figure 24 Mechanism of low adhesion in the train operation
(a) Crushed leaves, (b) Formation of graphite-like carbon, (c) Low adhesion and wheel-picking up

Taking into account the results presented in 3.1.1 and the previous work (12), the low adhesion is likely to be caused by two factors: graphite-like carbon and solid leaves. BBP suspension exhibited very low μ_L, and the leaf powder suspension showed the lowest traction levels at all the slip values, becoming black immediately after the application. The black layer had a graphite-like carbon structure; hence, the graphite-like carbon is highly likely to be the primary cause of low adhesion in cases of leaf contamination. On the other hand, lignin, which is a common organic component in leaves, has been studied as a functional additive of lubricants (38,39). Since the lignin was reported to improve anti-wear properties, the leaf powder itself could be the second factor of the long-term low adhesion.

Three hypotheses of the low adhesion mechanism were proposed by the authors: Bulk leaf, Adhered leaf film and Pectin gel (14). “Bulk leaf” theory is likely to be correct as the leaf can cause low adhesion. However, “Pectin gel” hypothesis could be incorrect; the graphite-like carbon is more persuasive to be the cause of low adhesion rather than the pectin gel on top of the leaf film. Moreover, pectin has been confirmed not to form a black precipitate with iron (12), and thus, pectin is unlikely to be the main cause. “Adhered leaf film” theory could be partially correct, although the moisture around the adhered leaf help to form a graphite-like carbon layer rather than simply softening the leaf film.

4.3 Bonding mechanism of leaf layers

Three hypotheses of the bonding mechanism were developed by the authors: sub- or supercritical water, Catalyst function of iron oxides and Cellulose or lignin adhesives theories (14). All of them were based on the idea that the high temperature due to the friction heat can make the bond stronger. However, this idea was found to be incorrect; the bonding energy decreased as the temperature increased, and the leaf film became patchy at 227 °C. This result clarified that the heat did not help to form a strong bond, and therefore, these three hypotheses are incorrect.

Moreover, the bonding energy of the leaf films created in this study was found to be small, since they were easily removed by nail-scratching. This small energy seems to contradict the report that the leaf film adheres to the rail (2). However, the laboratory-generated leaf film has been reported to be soft (3), supporting the finding in this study. Considering that the surface of the leaf film is covered with graphite-like carbon, the leaf film could be soft and easily shorn, rather than sticking to the rail.

Figure 25 depicts a schematic figure of the leaf film adhesion. Graphite has a low shear strength due to its layered-structure (40), and the graphite-like carbon layer on the leaf can be easily torn off by the shear stress. When some mechanical tool, such as a grinder and a scraper, attempts to remove the leaf film, only the upper layer is likely to be removed. This superficial removal might mislead to the understanding that the leaf film tightly adheres to the rail.

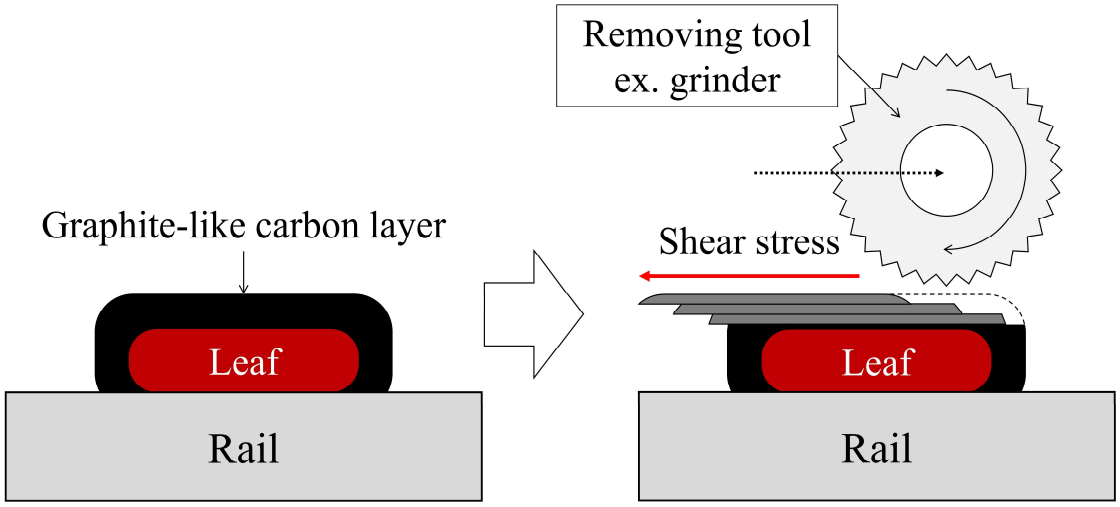

Figure 25 Mechanism of the leaf film adhesion

4.4 Potential prevention methods

In the field test conducted by the authors, train wheels were found to pick up leaves on the track and spread black residue for a long distance, around 10 metre (41). In other words, the leaf contamination could be minimised if the black leaf residue is removed from the wheel surface. Considering this observation, continuous tread braking during the autumn is proposed as a countermeasure in this study, which is very similar to drag braking for low adhesion due to snow (42).

Figure 26 illustrates the proposed method for prevention of leaf contamination. This method has two points to minimise the leaf contamination and improve adhesion levels: prevention of leaf film formation by mechanical removal and mitigation of low friction by braking temperature. Tread braking has been known to remove debris from a wheel surface and maintain surface roughness at a certain level. For instance, tread braking with a small braking force is used to remove snow on wheels in the winter, preventing the presence of snow between pads and wheels (42). Similar mechanical removal could happen in the case of leaf residue, which is possibly effective to stop the contamination from being spread.

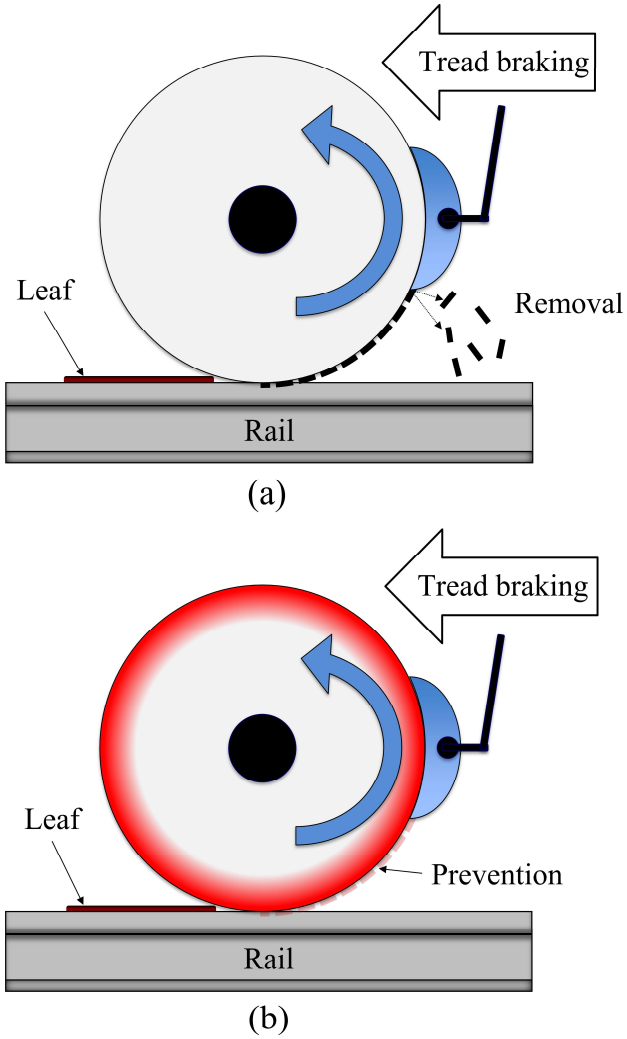

Figure 26 Proposed method for prevention of leaf contamination
(a) Mechanical removal, (b) Prevention of the chemical reaction

Moreover, tread braking is known to raise the surface temperature of the wheel (43). This fact indicates that tread braking could give enough thermal energy to mitigate the low adhesion due to leaf contamination. If the surface temperature is controlled around 240 °C by adjusting a braking force/pressure, it can maintain enough adhesion levels.

Negative aspects of this method are potential growth of thermal cracks on the wheel surface. When thermal cracks are present on the wheel surface, the wheel needs to be reprofiled at the maintenance centre, leading to an increase in maintenance costs. However, thermal cracks are generally grown above 400 °C, and no significant influence has been reported for thermal crack growth at around 240 °C (44). Another problem is excessive wear of wheels, which also leads to an increase in maintenance costs. Air pressure applied to the braking systems should be optimised to minimise the wear of wheels. To sum up, heat application by continuous tread braking could be a practical answer for leaf contamination, pushing all the risk to wheel-side and cutting the other costs.

On the other hand, there are some questions or issues to be addressed. For instance, it is unclear if high temperature only on the wheel side is enough to improve the traction. Another question is that the high temperature can affect the tribological behaviour of black leaf films, which have been already formed on the railway track. Before the actual application, further laboratory-based tests and field tests are necessary to examine to what extent this method is effective.

5. Conclusions

In this study, the temperature effect on the traction coefficient of leaf powder suspension was investigated using a twin disc machine to simulate the rolling-sliding contact between the wheel and rail. Leaf films were generated at different temperatures, and they were analysed by scratch test, laser Raman spectroscopy and Fourier transform infrared spectroscopy. Considering the acquired results, the drag braking with a small braking pressure was proposed as a potential countermeasure for the prevention of leaf films. The conclusions are shown as follows:

- Leaf powder suspension shows low traction coefficients in rolling-sliding conditions.
- Graphite-like carbon can be formed with leaves in wet conditions.
- This graphite-like carbon is likely to be the primary cause of low adhesion.
- Surface temperature proportionally improves the traction level of leaf powder suspension at 0.5 and 1 % slip.
- The surface temperature around 240 °C will be enough to meet the traction requirement.
- The leaf film created in this study did not have a high bonding energy
- Surface temperature is unlikely to affect the bonding strength of the leaf film.
- Continuous drag braking might be effective to prevent the spread of leaf film formation and to attain the necessary traction level.

To examine the proposed prevention method, further investigation regarding its effect should be conducted.

6. Acknowledgement

The authors would like to thank the University of Sheffield, UK, Rail Safety and Standards Board, UK, and East Japan Railway Company, Japan, for their financial support to carry out this research.

7. References

1. Edgley J. Managing Low Adhesion. Rail Delivery Group. 2018.

2. Fulford CR. Review of low adhesion research. A report published by Railways Safety and Standards Board. 2004;(May).

3. Poole W. Characteristics of Railhead Leaf Contamination. A report published by Railways Safety and Standards Board. 2007;

4. Network Rail. Our leaf-busting operation [Internet]. 2018. Available from: https://www.networkrail.co.uk/our-leaf-busting-operation/

5. E.A. Gallardo-Hernandez, R. Lewis. Twin disc assessment of wheel/rail adhesion. Wear. 2008;265(9–10):1309–16.

6. Arias-Cuevas O, Li Z, Lewis R, Gallardo-Hernández EA. Laboratory investigation of some sanding parameters to improve the adhesion in leaf-contaminated wheel–rail contacts. Proceedings of the Institution of Mechanical Engineers, Part F: Journal of Rail and Rapid Transit. 2010;224(3):139–57.

7. Omasta M, Machatka M, Smejkal D, Hartl M, Křupka I. Influence of sanding parameters on adhesion recovery in contaminated wheel–rail contact. Wear. 2015;322–323:218–25.

8. Lewis R, Dwyer-Joyce RS. Wear at the wheel/rail interface when sanding is used to increase adhesion. Proceedings of the Institution of Mechanical Engineers Part F: Journal of Rail and Rapid Transit. 2006;220(1):29–41.

9. Vasić G, Franklin F, Kapoor A, Lučanin V. Laboratory simulation of low adhesion leaf film on rail steel. International Journal of Surface Science and Engineering. 2008;2:84–97.

10. Global Railway Review. To combat leaves on the line, specially designed trains will travel 120,000 miles. 2018; Available from: https://www.globalrailwayreview.com/news/74055/leaves-line-network-rail-safety/

11. Hyde P, Fletcher DI, Kapoor A, Richardson S. Full scale testing to investigate the effect of rail head treatments of differing pH on railway rail leaf films. In: The World Congress on Railway Research. 2008. p. 18–22.

12. Ishizaka K, Lewis SR, Hammond D, Lewis R. Chemistry of black leaf films synthesised using rail steels and their influence on the low friction mechanism. RSC Advances. 2018;8(57):32506–21.

13. Boles JS, Crerar DA, Grissom G, Key TC. Aqueous thermal degradation of gallic acid. Geochimica et Cosmochimica Acta. 1988;52(2):341–4.

14. Ishizaka K, Lewis SR, Lewis R. The low adhesion problem due to leaf contamination in the wheel/rail contact: Bonding and low adhesion mechanisms. Wear. 2017;378–379:183–97.

15. Li Z, Arias-Cuevas O, Lewis R, Gallardo-Hernández EA. Rolling–Sliding Laboratory Tests of Friction Modifiers in Leaf Contaminated Wheel–Rail Contacts. Tribology Letters. 2009;33(2):97–109.

16. Lewis SR, Lewis R, Cotter J, Lu X, Eadie DT. A new method for the assessment of traction enhancers and the generation of organic layers in a twin-disc machine. Wear. 2016;366–367:258–67.

17. Arias-Cuevas O, Li Z, Lewis R, Gallardo-Hernández EA. Rolling-sliding laboratory tests of friction modifiers in dry and wet wheel-rail contacts. Wear. 2010;268(2–3):543–51.

18. Polach O. Creep forces in simulations of traction vehicles running on adhesion limit. Wear. 2005;258(7–8):992–1000.

19. Olofsson U, Zhu Y, Abbasi S, Lewis R, Lewis SR. Tribology of the wheel–rail contact – aspects of wear, particle emission and adhesion. Vehicle System Dynamics. 2013;51(7):1091–120.

20. Lewis R, Olofsson U. Wheel-rail Interface Handbook. 2009. 32–57 p.

21. Gallardo-Hernandez EA, Lewis R, Dwyer-Joyce RS. Temperature in a twin-disc wheel/rail contact simulation. Tribology International. 2006;39(12):1653–63.

22. Ollivier B, Matthews A. Adhesion of diamond-like carbon films on polymers: An assessment of the validity of the scratch test technique applied to flexible substrates. Journal of Adhesion Science and Technology. 1994;8(6 pt 3):651–62.

23. Das S, Lahiri D, Lee DY, Agarwal A, Choi W. Measurements of the adhesion energy of graphene to metallic substrates. Carbon. 2013;59:121–9.

24. Keshri AK, Lahiri D, Agarwal A. Carbon nanotubes improve the adhesion strength of a ceramic splat to the steel substrate. Carbon. 2011;49(13):4340–7.

25. Lahiri I, Lahiri D, Jin S, Agarwal A, Choi W. Carbon nanotubes: How strong is their bond with the substrate? ACS Nano. 2011;5(2):780–7.

26. Bull SJ, Rickerby DS, Matthews A, Leyland A, Pace AR, Valli J. The use of scratch adhesion testing for the determination of interfacial adhesion: The importance of frictional drag. Surface and Coatings Technology. 1988;36(1–2):503–17.

27. Ferrari AC, Robertson J. Interpretation of Raman spectra of disordered and amorphous carbon. Phys Rev B. 2000;61(20):95–107.

28. de Faria DLA, Silva SV, de Oliveira MT. Raman microspectroscopy of some iron oxides and oxyhydroxides. Journal of Raman Spectroscopy. 1997;28(February):873–8.

29. Nakahara T, Baek KS, Chen H, Ishida M. Relationship between surface oxide layer and transient traction characteristics for two steel rollers under unlubricated and water lubricated conditions. Wear. 2011;271(1–2):25–31.

30. Tuinstra F, Koenig JL. Raman Spectrum of Graphite. The Journal of Chemical Physics. 1970;53(3):1126–30.

31. Saravanan M, Ganesan M, Ambalavanan S. An in situ generated carbon as

integrated conductive additive for hierarchical negative plate of lead-acid battery. Journal of Power Sources. 2014;251:20–9.

32. Williams DH, Ian Fleming. Spectroscopic Methods in Organic Chemistry. Fourth. London: McGraw-Hill; 1989.

33. Cann PM. The “leaves on the line” problem - A study of leaf residue film formation and lubricity under laboratory test conditions. Tribology Letters. 2006;24(2):151–8.

34. Yang H, Yan R, Chen H, Lee DH, Zheng C. Characteristics of hemicellulose , cellulose and lignin pyrolysis. Fuel. 2007;86:1781–8.

35. Chen H, Ban T, Ishida M, Nakahara T. Adhesion between rail/wheel under water lubricated contact. Wear. 2002;253(1–2):75–81.

36. Chen H, Ban T, Ishida M, Nakahara T. Experimental investigation of influential factors on adhesion between wheel and rail under wet conditions. Wear. 2008;265(9–10):1504–11.

37. Xiaowei L, Suyuan Y, Xuanyu S, Shuyan H. The influence of roughness on tribological properties of nuclear grade graphite. Journal of Nuclear Materials. 2006;350(1):74–82.

38. Mu L, Shi Y, Guo X, Ji T, Chen L, Yuan R, et al. Non-corrosive green lubricants: strengthened lignin-[choline][amino acid] ionic liquids interaction via reciprocal hydrogen bonding. RSC Advances. 2015;5(81):66067–72.

39. Mu L, Wu J, Matsakas L, Chen M, Vahidi A, Grahn M, et al. Lignin from hardwood and softwood biomass as a lubricating additive to ethylene glycol. Molecules. 2018;23(3):1–10.

40. Stachowiak GW, Batchelor AW. Engineering tribology. Fourth. Oxford: Elsevier/Butterworth-Heinemann; 2014.

41. Lanigan J, Krier P, Buckley-Johnstone L, White B, Ishizaka K, Cooke J, et al. Towards a Field Test Methodology for Locomotive Brake Testing Using a Representative Low Adhesion Simulation. In: 11th International Conference on Contact Mechanics and Wear of Rail/Wheel Systems. Delft, The Netherlands; 2018.

42. Olofsson U, Sundh J, Bik U, Nilsson R. The influence of snow on the tread braking performance of a train: A pin-on-disc simulation performed in a climate chamber. Proceedings of the Institution of Mechanical Engineers, Part F: Journal of Rail and Rapid Transit. 2016;230(6):1521–30.

43. Vernersson T. Temperatures at railway tread braking. Part 1: modelling. Proceedings of the Institution of Mechanical Engineers, Part F: Journal of Rail and Rapid Transit. 2007;221:167–82.

44. Handa K, Morimoto F. Influence of wheel/rail tangential traction force on thermal cracking of railway wheels. Wear. 2012;289:112–8.